

Rate Theories and Puzzles of Hemeprotein Kinetics

Hans Frauenfelder and Peter G. Wolynes

Chemical reactions govern all aspects of biological processes, from enzyme catalysis to transfer of charge, matter, and information. Any deep understanding of biological reactions must be based on a sound theory of chemical reaction dynamics. Most of the knowledge of reaction dynamics, however, has been deduced from studies of two-body interactions of small molecules in the gas phase (1). In contrast to this simple system, biomolecules provide a complex

environment, thus no explicit attention need be paid to the dynamics of the changing electronic structure. In that case, a picture of the reaction dynamics based on a single adiabatic potential-energy surface is appropriate. When the spins of the reactants change or when long-range electron transfer is involved, however, the changes in electronic structure may be slower than the nuclear motion. The characteristics of the electronic motion, then, are important in determining the

Summary. The binding of dioxygen and carbon monoxide to heme proteins such as myoglobin and hemoglobin has been studied with flash photolysis. At temperatures below 200 K, binding occurs from within the heme pocket and, contrary to expectation, with nearly equal rates for both ligands. This observation has led to a reexamination of the theory of the association reaction taking into account friction, protein structure, and the nature of electronic transitions. The rate coefficients for the limiting cases of large and small friction are found with simple arguments that use characteristic lengths and times. The arguments indicate how transition state theory as well as calculations based on nonadiabatic perturbation theory, which is called the Golden Rule, may fail. For ligand-binding reactions the data suggest the existence of intermediate states not directly observed so far. The general considerations may also apply to other biomolecular processes such as electron transport.

but highly organized environment that can affect the course of the reaction. Fortunately, the complexity imparts a richness of phenomena that allows the examination of fundamental aspects of reaction dynamics. Biomolecules, in particular heme proteins, are an excellent laboratory as shown, for example, by the observations of nuclear tunneling in them (2-4).

Most reactions involve motion of the nuclei of the reacting species and changes in their electronic structure. For many reactions the electronic structure adiabatically follows the nuclear mo-

tion, and a theory of the nonadiabatic transition from one electronic state to another is needed. Such a theory has been used as the basis of most treatments of biological electron transfer (5). Since kinetic control is at the heart of many biological processes, an assessment of the relative importance of nuclear and electronic motions is desirable.

The binding of dioxygen (O₂) and carbon monoxide (CO) to heme proteins is a situation where the problem can be studied in detail. In this article, we discuss these reactions with the aim of constructing a qualitative framework for un-

derstanding the general issue of nuclear and electronic motions in biomolecular reactions. In this analysis, we consider recent ideas on the influence of dissipation and fluctuations on reaction dynamics and show the limitations of transition state theory in complex systems. Attempts to understand heme reactions have been made before, notably by Jortner and Ulstrup (6) and by Hopfield and his co-workers (7), who have used theories of nonadiabatic transitions. We show that an approximation of adiabatic behavior may be closer to reality. The analysis of the specific reactions leads to general conclusions that may be applicable to other reactions in biomolecules and in condensed phases.

Binding of O₂ and CO to Heme Proteins

The "laboratory" for studying the binding reaction is shown in Fig. 1, a schematic cross section of a heme protein, for instance myoglobin or a separated hemoglobin chain. Flash photolysis experiments suggest that ligand binding occurs through a complex path: the ligand, for instance O₂, enters the protein matrix from the solvent, moves through the matrix into the heme pocket, and binds covalently to the heme iron (8). The formation of the covalent bond between the ligand and the iron is the rate-limiting step (9). We will concern ourselves with this step, not with the motion from the solvent to the pocket.

The initial state (called state B) and the final state (called state A) in the bond formation are structurally and spectroscopically well characterized (10). The spatial structures of the CO- and O₂-bound species are similar. Before bond formation, the heme iron has spin 2; it lies about 0.5 Å out of the mean heme plane; and the heme is domed. In the bound state, A, the spin is zero; the iron has moved closer to the heme plane; and the heme is nearly planar. The best current descriptions of the electronic structure of the oxy and the carbon monoxy species are, however, different (11). The free CO molecule in state B has closed

Hans Frauenfelder is a professor of physics and Peter Wolynes is a professor of chemistry at the University of Illinois, Urbana-Champaign 61801.

Table 1. Values of the peak activation enthalpy, H_{BA}^{peak} , and the preexponential term, A_{BA} , for the binding of O_2 and CO to three heme proteins.

Heme protein	H_{BA}^{peak} (kJ mol ⁻¹)		log (A_{BA}/sec^{-1})	
	O ₂	CO	O ₂	CO
Myoglobin	10.2	11.0	9.3	9.2
β^A	3.2	4.0	9.8	9.4
β^Z	1.5	2.0	8.8	8.8

shells and is in the singlet configuration $^1\Sigma^+$. Free O_2 , in contrast, is in the triplet state $^3\Sigma_g$ and has unpaired electrons outside a closed shell. The bound states of the two ligands consequently differ. The CO complex is described according to ligand field theory as being a $(t_{2g})^6$ ferrous iron, coordinated with the strong-field ligand CO and the auxiliary ligands of the protein. The O_2 complex is most easily characterized via valence bond theory as a biradical in which the ferrous iron has orbital occupations of intermediate spin $(e_g)^1(t_{2g})^5$ and is bonded to the triplet O_2 . The spins on the iron and oxygen are paired through an antiferromagnetic superexchange interaction, which results in an overall singlet state.

Given the difference in electronic structure, it is surprising to find that O_2 and CO bind similarly. The bond formation $B \rightarrow A$ has been studied at temperatures between about 40 and 160 K (8). The binding process is not exponential in time. This observation is explained by postulating that each protein molecule can assume a large number of slightly different conformational substates, each with a different activation enthalpy H_{BA} for the transition $B \rightarrow A$, and that below 200 K each molecule is frozen into a particular substate. We denote with $g(H_{BA}) dH_{BA}$ the probability of finding a protein molecule with activation barrier between H_{BA} and $H_{BA} + dH_{BA}$ and assume an Arrhenius expression $k_{BA}(H_{BA}, T) = A_{BA} \exp(-H_{BA}/RT)$, for the rate coefficient $k_{BA}(H_{BA}, T)$ where T is the absolute temperature. The experimental data then determine A_{BA} and $g(H_{BA})$. Figure 2 gives $g(H_{BA})$ for the binding of O_2 and CO to myoglobin (Mb) and the separated β chains of normal human hemoglobin (β^A) and the mutant hemoglobin Zürich (β^Z) (8, 9, 12, 13). All the distributions have essentially the same shape but different peak enthalpies, H_{BA}^{peak} . Values of H_{BA}^{peak} and A_{BA} are listed in Table 1. The preexponential factors, the peak enthalpies, and the distribution of activation enthalpies are similar for O_2 and CO binding to a given protein (Fig. 2 and Table 1).

The data presented in Fig. 2 and Table 1 are the center of the puzzle of heme-

protein kinetics: if the electronic structures and the changes in spin state are so different for CO and O_2 , why are the preexponential factors and the enthalpy distributions so similar? The adiabaticity or nonadiabaticity of the binding reaction should be reflected in these data. In both cases a spin change mediated through the weak spin-orbit interaction is necessary, and thus a nonadiabatic process is possible. For O_2 a net spin change of 1 occurs, and only a first-order spin-orbit interaction is needed. The spin prohibition should be so weak that the process would be adiabatic. In the CO case, a net spin change of 2 is involved, necessitating the intervention of a electronically slower second-order spin-orbit interaction if the transition is direct. Binding of CO consequently is expected to be nonadiabatic.

The puzzle is compounded by a consideration of the preexponential A_{BA} . The values in Table 1 show that the value of A_{BA} for O_2 and CO in all three heme proteins is about 10^9 sec^{-1} , smaller by approximately a factor of 10^3 than the canonical value of 10^{12} sec^{-1} at about 100 K. The smallness of A_{BA} is sometimes taken as evidence for nonadiabaticity. The fact that A_{BA} is the same for O_2 and CO casts doubt on this interpretation, and the ratio of the preexponential factors A_{BA} and A_{AB} strengthens the doubts. The rate of the transition $B \rightarrow A$ is inversely proportional to the number

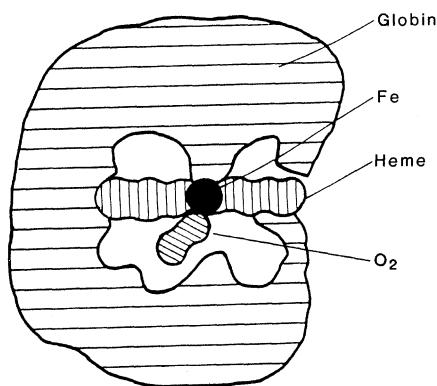


Fig. 1. Schematic cross section of a heme protein. The small ligand, O_2 , is shown bound to the heme iron in the heme pocket on the distal side.

of states, n_B , in the initial state B. If the Boltzmann relation $S = k_B \ln n$, where S is the entropy and k_B the Boltzmann constant, is applied, the ratio of preexponential factors for the transitions $A \rightarrow B$ and $B \rightarrow A$ can be written as $A_{AB}/A_{BA} = n_B/n_A = e^{(S_B - S_A)/k_B}$. For oxymyoglobin (MbO_2), A_{AB} can be determined directly. The dissociation rate for MbO_2 has been measured with a replacement reaction after flash photolysis from 260 to 320 K (14). With a simple kinetic analysis (9) $k_{AB}(T)$ can be found. An Arrhenius plot then yields $H_{AB} = 79 \text{ kJ mol}^{-1}$ and $A_{AB} = 2 \times 10^{15} \text{ sec}^{-1}$ so that $A_{AB}/A_{BA} \approx 10^6$ or $(S_B - S_A)/k_B \approx 14$. [Such an entropy loss in going from B to A is reasonable. In B, the ligand occupies a volume of about 30 \AA^3 (9); the corresponding loss of translational entropy accounts for $8k_B$ (15). The loss of rotational entropy of the ligand and the spin change of the iron can account for the remaining $6k_B$ (16).] Equilibrium data indicate a similar entropy loss in the last step of CO binding. If one half of the entropy loss in going from B to A occurs between the pocket, that is, the B state, and the transition state, the smallness of A_{BA} is attributable to the entropy drop alone, and there is no need for a small, dynamic preexponential factor, which would be symptomatic for nonadiabaticity. We must entertain the possibility that both CO and O_2 binding occur by means of partially or fully adiabatic transitions.

The expectation that the step $B \rightarrow A$ is nonadiabatic for the binding of CO arises from the conventional adiabaticity criterion, which we will discuss in the next section. Two phenomena can change the criterion, friction (dissipation) and the existence of intermediate states. Friction can account for a small preexponential term and increase the time that the system spends in the transition state, thus rendering a nonadiabatic transition adiabatic. The entropy argument, however, makes a large reduction of the preexponential factor through friction unlikely. Nevertheless, we will discuss the effect of friction in the following sections. The explanation of adiabaticity through the existence of intermediate states is favored by two experimental observations, the pressure dependence of the kinetics and the results from low-temperature infrared spectroscopy. Studies of the $B \rightarrow A$ transition at temperatures between 60 and 160 K with pressures up to 2 kbar show that k_{BA} increases with pressure for the binding of CO to myoglobin, decreases with pressure for the binding of O_2 to myoglobin, and is nearly pressure-independent for

the binding of CO to protoheme (17). These observations are consistent with the pressure dependencies measured for the overall binding rates at 300 K (18). The different pressure dependencies of CO and O₂ are hard to reconcile with the idea that the transition B → A is a direct one. The occurrence of intermediate states is also suggested by the observation with infrared spectroscopy of CO binding at low temperatures (19).

Adiabatic and Nonadiabatic

Potential Surfaces

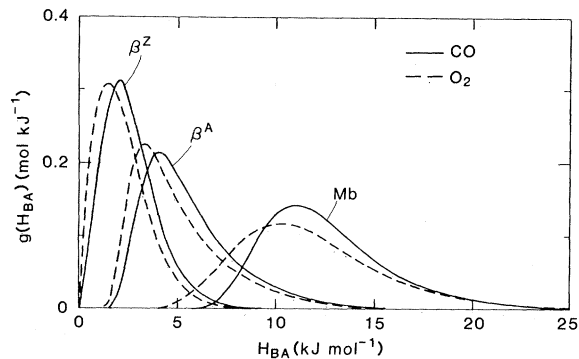
To provide a theoretical framework for discussing the problems outlined in the previous section, we will first recapitulate the differences between adiabatic and nonadiabatic transitions in simple reactions. In chemical reactions, both electrons and nuclei move. Because of the mass difference between electrons and nuclei, we can consider the nuclei at any moment to be fixed and obtain energy levels for the electronic motion in the fixed field of the nuclei as functions of the distance between the nuclei (the Born-Oppenheimer approximation). As an example, we show in Fig. 3 the potential energy curves for the reaction of CO with the heme group in a one-dimensional model in two different approximations. We assume that only two electronic states exist, the bound state *s* (for singlet) and the unbound state *q* (for quintuplet). If the matrix element V_{sq} connecting the two states is zero, the resulting diabatic energy curves (Fig. 3a) cross each other. If the interaction between the two states is not zero, the curves "repel" each other (Fig. 3b) (20). The splitting (least distance) between the two curves is given by

$$\Delta = 2 |V_{sq}|$$

The curve that starts out as *q* at large values of *r* changes character in the mixing region and becomes *s* at small values of *r*. In the mixing region, both curves are superpositions of *s* and *q*. Some confusion occasionally arises in the interpretation of diagrams like those in Fig. 3: the curves do not represent potentials that are used in the Schrödinger equation to determine energy levels; indeed they are the energy levels (or energy surfaces) as a function of the distance *r*.

We now consider the dynamics of the association process in terms of Fig. 3, using a semiclassical model in which the nuclei move classically and the electronic state adjusts to the changing nuclear coordinates. Assume the system starts

Fig. 2. Distribution function, $g(H_{BA})$, for the binding of CO (solid lines) and O₂ (dashed lines) to three monomeric heme proteins.



out in state B. Only through the V_{sq} coupling can a transition occur; if $V_{sq} = 0$, the system will remain in state B because the electronic state cannot change even if the nuclear coordinates, through their thermal motion, find themselves in the A configuration. Transitions outside of the mixing region can be neglected (21); the transition B → A depends on the passage of nuclei through the crossing region. If V_{sq} is very large compared to the kinetic energy of nuclear motion, $k_B T$, the upper electronic state will be thermally inaccessible ($\Delta \gg k_B T$), and the nuclei will move according to the lower state, adiabatic potential curve. The electronic dynamics can be ignored, except in so far as it determines the adiabatic surface. When $\Delta \lesssim k_B T$, thermodynamic considerations alone do not determine whether the electronic state can change. Depending on the relative time scale of electronic and nuclear motion, the system can either remain in state *q*, move along the dashed diabatic curve in Fig. 3b, and reach the upper surface, or it can undergo a transition *q* → *s* and move along the solid adiabatic curve. To obtain a criterion characterizing adiabaticity we use the uncertainty relation: if the energy uncertainty of the system in the mixing region is small compared to the splitting, Δ , the system will remain on the lower surface and the transition will be adiabatic. The energy uncertainty is given by \hbar/τ_{LZ} , where \hbar is Planck's constant divided by 2π and τ_{LZ} is the time spent in the mixing

region, which is called the Landau-Zener region. If the system moves through the mixing region with constant velocity *v* and if transitions can occur over a region of length ℓ_{LZ} , τ_{LZ} is given by

$$\tau_{LZ} = \ell_{LZ}/v$$

From Fig. 3b, ℓ_{LZ} is approximately given by

$$\ell_{LZ} = \frac{\Delta}{|F_2 - F_1|} \quad (1)$$

where the forces F_1 and F_2 are the slopes of the diabatic curves at the avoided crossing r_0 . The adiabaticity parameter γ_{LZ} , defined as the ratio of the splitting Δ to the energy uncertainty \hbar/τ_{LZ} , can be written as

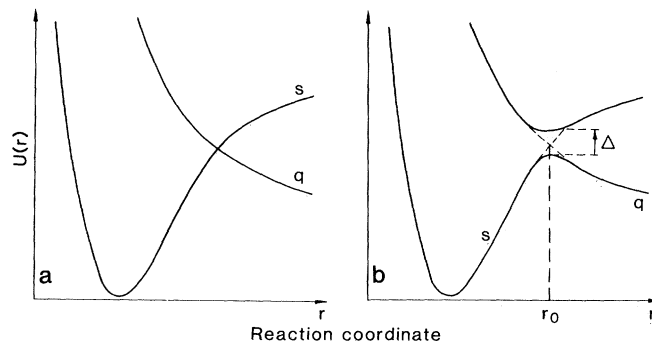
$$\gamma_{LZ} = \frac{\Delta}{\hbar/\tau_{LZ}} = \frac{\ell_{LZ}\Delta}{\hbar v} = \frac{\Delta^2}{\hbar v |F_2 - F_1|} \quad (2)$$

If $\gamma_{LZ} \gg 1$, the transition is adiabatic. If $\gamma_{LZ} \lesssim 1$, the system can remain on the diabatic surface and reach the upper state. Not every crossing through the mixing region then results in a transition from the initial state B to the final state A. The probability *P* for the electronic structure to change on a single crossing, that is, for the system to stay on the adiabatic surface, has been calculated by Landau (22), Zener (23), and Stueckelberg (24) as

$$P = 1 - \exp(-\pi\gamma_{LZ}/2) \quad (3)$$

This expression verifies the argument given above; if $\gamma_{LZ} \gg 1$, $P = 1$, and

Fig. 3. Schematic representation of the potential energy curves for the reaction of CO with the heme iron: (a) diabatic energy levels; (b) adiabatic energy levels. Here *s* denotes the singlet state, and *q* the quintuplet state; transitions *s* → *q* are forbidden in (a).



the transition is adiabatic. If $\gamma_{LZ} \ll 1$, the following expression is obtained:

$$P = \frac{\pi}{2} \gamma_{LZ} = \frac{\pi}{2} \frac{\Delta^2}{\hbar v |F_2 - F_1|} \quad (4)$$

The probability is proportional to Δ^2 , which is the hallmark of a highly nonadiabatic reaction. The dependence on Δ^2 is also obtained in derivations of rate coefficients from nonadiabatic perturbation theory, which is called the Golden Rule, in which Δ is treated as a small perturbation causing the electronic transition.

Transition State Theory of Adiabatic Reactions

Even when a reaction takes place adiabatically on a single potential surface, the determination of the rate coefficient requires a consideration of the dynamics of configurational rearrangement. The simplest theory of rate coefficients is the transition state theory (TST) (1). Its keystone is the assumption that a typical reactive trajectory crosses the barrier from reactant to product only once before being trapped for a very long time; later recrossings are unrelated events. This assumption reduces the calculation of a rate coefficient to a consideration of the equilibrium concentration of activated configurations. To find the TST rate, we consider an adiabatic one-dimensional reaction represented by the lower solid curve in Fig. 3b and neglect transitions $A \rightarrow B$. The number of systems that move from B to A per unit time is given by $dN_B/dt = kN_B$, where dN_B/dt is the rate, k is the rate coefficient, and N_B is the number of systems in state B. If the system moves over the barrier with average thermal velocity

$$v = (2k_B T / \pi m)^{1/2}$$

where m is the effective mass associated with the reaction coordinate, and without being hindered (a ballistic transition), the rate is essentially the same as that given by the kinetic theory of gases for effusive flow through an orifice,

$$\frac{dN_B}{dt} = \frac{1}{2} v N^\ddagger \quad (5)$$

$N^\ddagger dx$ is the number of systems within a range dx around the transition state configuration. The factor 1/2 arises because only one half the particles are moving toward A. The Boltzmann distribution determines the fraction of molecules in the transition state:

$$\frac{N^\ddagger}{N_B} = \frac{\exp(-H^\ddagger/k_B T)}{\int_{r \in B} dr \exp[-U(r)/k_B T]} \quad (6)$$

where H^\ddagger is the enthalpy of activation (H_{BA}), r is the position on the reaction coordinate, and $U(r)$ is the potential energy as a function of the reaction coordinate. If the barrier is high compared to $k_B T$ and the potential in B is harmonic,

$$U(r) = \frac{1}{2} m \omega_B^2 (r - r_B)^2$$

where ω_B is the frequency of motion in the B well. The integration in Eq. 6 can be performed, and the result combined with Eq. 5 yields the transition-state rate coefficient k_{TST} :

$$\frac{dN_B}{dt} = -k_{TST} N_B \quad k_{TST} = \frac{\omega_B}{2\pi} e^{-H^\ddagger/k_B T} \quad (7)$$

Entropy and Friction in Chemical Reactions

So far we have treated reactions as two-body collisions in one dimension. In reality a biochemical reaction takes place in a condensed phase and involves potential energy surfaces that are multidimensional. In such complex reactions, however, it is often useful to consider one or a few coordinates of motion as the most important in determining the reaction rate. This reduced description of the reaction coordinates entails the introduction of two new concepts, one a static modification of potential energy surfaces due to entropy and the other a dynamical effect loosely described as friction. The mathematics of this reduction in level of description has been worked out for processes occurring on a single potential surface when the nuclear motion is classical. Although the corresponding development for multiple energy surfaces is somewhat problematic, the approach seems adequate for the present discussion, in which we assume classical nuclear motion.

The introduction of entropy is straightforward. We continue to use the diagram Fig. 3b, but interpret it as a plot of the Gibbs free energy $G(r)$ as a function of the reaction coordinate that has been singled out. The activation enthalpy H^\ddagger in Eq. 7 is replaced by the Gibbs free energy of activation, $G^\ddagger = H^\ddagger - TS^\ddagger$, where S^\ddagger is the entropy of activation and e^{S^\ddagger/k_B} is the ratio of the number of states in the transition state to that in the initial state. The entropy counts the number of states available in the disregarded, or "invisible," coordinates when the reaction coordinate has a fixed value. Thus if the entropy is smaller in the transition state than in the reactant the rate is diminished (just as the rate of getting billiard balls into the pockets de-

creases as the pocket area decreases).

One-dimensional Newtonian motion on the free energy surface does not faithfully imitate the motion of the reaction coordinate. The invisible coordinates have a profound dynamical effect on this motion and, through a breakdown of the TST dynamical assumption, can dramatically affect the rate. To understand the dynamical effect of the invisible coordinates we note that the energy and momentum of the entire system, protein plus environment, are, of course, conserved. If we could treat the entire system without approximations, all dynamical effects would be incorporated, and there would be no need to introduce friction. The separation into a reaction coordinate and invisible coordinates changes the way in which we treat the system. The invisible coordinates exchange energy and momentum with the reaction coordinate. Energy and momentum of the reaction coordinate alone are not conserved; the reaction coordinate can gain or lose energy and momentum. The effect of this exchange on the reaction coordinate is called friction. Friction is essential for the trapping of the system in the product state. A necessary concomitant of friction is the fluctuation forces arising also from the ignored coordinates (25). When friction is large the motion along the reaction coordinate looks like a Brownian motion or a random walk, not the motion of a particle subject to conservative forces. Friction can be roughly characterized by a velocity autocorrelation time τ_v , which is inversely proportional to the friction coefficient ζ ,

$$\tau_v = m/\zeta \quad (8)$$

Here again m is the effective mass. In a liquid, friction is approximately related to the viscosity by Stokes law as

$$\zeta \approx 6\pi\eta a \quad (9)$$

where η is the coefficient of viscosity and a is a characteristic linear distance. Friction and fluctuations were taken into account in 1940 by Kramers, who used the Fokker-Planck equation to treat reactions as the escape of particles from a one-dimensional potential well (26). For a long time, Kramers' work was only appreciated by a few theoreticians (27). Recently, however, his ideas have resurfaced in much theoretical (28) and experimental work (14, 29) on kinetics in condensed phases. The frictional effects on the rate are contained in a transmission coefficient, κ , which represents the fact that even when the system is poised at the transition state and is moving toward product formation, it will not

necessarily get there, because fluctuations in the other coordinates can exert forces that reverse the direction of motion. Thus, in a typical reactive path, the reactants do not go directly from one side of the well to the other but rather may cross the transition region many times, tottering back and forth before reacting. A rate coefficient counts the number of successful trajectories. For an adiabatic reaction, TST counts each of the forward crossings on a single trajectory as contributing to the rate. The TST thus overestimates the rate coefficient by a factor equal to the number of times, $(N_c + 1)/2$, that a typical trajectory crosses the col before falling to one side or the other. The transmission coefficient is roughly the inverse of the number of forward crossings,

$$\kappa = 2/(N_c + 1)$$

Since N_c can be large, this argument shows the error in the belief that the transmission coefficient cannot be smaller than $1/2$ because the system must fall into either the reactant or the product well.

The fundamental results of Kramers and the corroborating modern analyses can be stated simply. At low friction the transmission factor is proportional, and at high friction inversely proportional, to the friction coefficient. In the intermediate regime, κ depends somewhat on the potential surface topography and frictional mechanism, but the value predicted by TST (when tunneling is neglected) is an upper limit that can be significantly in error (30). These results are summarized in the graph of transmission factors in Fig. 4.

The Reaction Rate at the Low and High Friction Limits

Figure 4 shows the two Kramers regimes of the reaction rate, the underdamped one with $k \propto \zeta$ and the overdamped one with $k \propto 1/\zeta$. The rate coefficient reaches a maximum at a value

$$\zeta_{\text{crit}} = dm\omega \quad (10)$$

where d is a numerical constant that depends on the energy surface and the damping mechanism but is smaller than 1 (28, 31). With the Stokes relation (9) and $d = 1$, Eq. 10 becomes

$$\eta_{\text{crit}} = (1/3)(m/a)(\omega/2\pi)$$

The typical values of $m/a = 2 \times 10^{-15}$ g cm⁻¹ and $\omega/2\pi = 10^{13}$ sec⁻¹ yield $\eta_{\text{crit}} = 7$ millipoise (mP). Water at 300 K has a viscosity of 8.5 mP, so we expect most protein reactions to be overdamped.

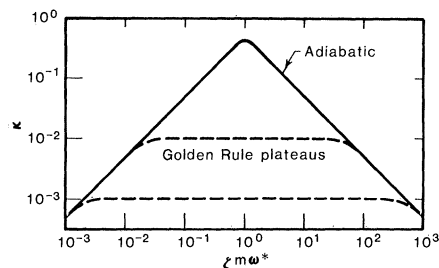


Fig. 4. The transmission factor κ as a function of the friction coefficient ζ (in units of $m\omega^*$). The solid line indicates the adiabatic Kramers curve. The dashed lines correspond to the situation where the Landau-Zener factor is smaller than 1.

Whereas the calculation of the reaction rate over the entire range of friction is difficult (26–28, 31), the limiting cases $\zeta \ll \zeta_{\text{crit}}$ and $\zeta \gg \zeta_{\text{crit}}$ can be treated by using simple physical arguments based on the two characteristic lengths in the problem. The first length is the mean free path, λ , the average distance before the coordinate reverses its direction of motion. From Eq. 8, λ is related to the velocity autocorrelation time τ_v or the friction ζ by

$$\lambda = v_{\text{rms}} \tau_v \approx (2mk_B T)^{1/2}/\zeta \quad (11)$$

where v_{rms} is the root-mean-square velocity. The second relevant length is the size of the transition region, ℓ_{TS} , defined by the condition that the energy in this region is within $k_B T$ of the transition state energy. For a parabolic Gibbs energy barrier with curvature $m(\omega^*)^2$ at the col, ℓ_{TS} is given by

$$\ell_{\text{TS}} = 2[2k_B T/m(\omega^*)^2]^{1/2} \quad (12a)$$

where ω^* is the undamped frequency of motion at the top of the transition barrier. For a cusp-like barrier, as occurs in surface crossings, ℓ_{TS} is given by

$$\ell_{\text{TS}} = k_B T \left(\frac{1}{|F_2|} + \frac{1}{|F_1|} \right) \quad (12b)$$

The character of the transition is determined by the ratio λ/ℓ_{TS} , given by Eqs. 11 and 12 as

$$\lambda/\ell_{\text{TS}} = m\omega^*/2\zeta \quad (13)$$

Equation 10 implies that the motion in the transition state is critically damped if $\lambda \approx \ell_{\text{TS}}$. If $\lambda \gg \ell_{\text{TS}}$, the crossing through the transition region will be ballistic; if $\lambda \ll \ell_{\text{TS}}$, the system will undergo many collisions in the transition state. We will now discuss the two extremes in more detail.

Low friction. If the friction is low, the system, on leaving the transition state, will not lose sufficient energy to drop into an energy well but will bounce off the other side and recross the energy

barrier. If τ_r is the time to traverse the well and τ_E the time to lose approximately the energy $k_B T$, the system will go back and forth across the barrier roughly $N_c = \tau_E/\tau_r$ times before being deactivated. In general, τ_E is proportional to the velocity autocorrelation time τ_v , Eq. 8, with a proportionality coefficient that depends on the friction mechanism. For the Fokker-Planck model used by Kramers,

$$\tau_E = \tau_v (H^\ddagger/k_B T)^{-1/2}$$

The transmission factor

$$\kappa = N_c^{-1} = \tau_r/\tau_E$$

is thus, in general, proportional to the friction as illustrated in the left branch of the curve in Fig. 4. The same result is obtained by considering the time it takes to activate a system that is initially in well B. Activation and deactivation are related by microscopic reversibility. For a one-dimensional system, τ_r is of the order of ω_B^{-1} . If the reaction coordinate is coupled to internal degrees of freedom (that are not counted as contributing to friction), the system may get lost in the multidimensional phase space before re-finding the passageway, and τ_r may be much longer than ω_B^{-1} . The behavior of the reaction rate at low friction consequently depends on details of the multidimensional potential surface.

High friction. When the friction is high, energy flow into and out of the reaction coordinate is assured and not rate-limiting. Instead the high friction leads to Brownian motion of the system in the transition region and the system crosses the top of the barrier many times. Of the time spent in the transition region a fraction, λ/ℓ_{TS} , is spent within a mean free path of the top. The system's total number of velocity reversals while remaining in the transition region is given by $N = (\ell_{\text{TS}}/\lambda)^2$, the relation for a random walk. Thus, there are typically

$$N_c = (\lambda/\ell_{\text{TS}}) N = \ell_{\text{TS}}/\lambda$$

crossings at the top of the barrier and

$$\kappa = 2/(N_c + 1) \approx 2\lambda/\ell_{\text{TS}}$$

Combining $\kappa = 2\lambda/\ell_{\text{TS}}$ with Eqs. 7 and 13, we find the rate coefficient at the high-damping limit becomes

$$k(T, \zeta) = \frac{m\omega^*\omega_B}{2\pi\zeta} e^{-G^\ddagger/k_B T} \quad (14)$$

Here we have replaced H^\ddagger by the Gibbs free energy of the activated state, G^\ddagger . Equation 14 is the relation Kramers found at the high-damping limit (26). (This limit is sometimes called the "diffusion limit." Diffusion here refers to the Brownian passage over the col and not to

the ordinary diffusion that governs “diffusion-controlled” bimolecular reactions.)

The approach of Kramers is a more appropriate description of biomolecular reactions than is TST. One point, in particular, requires an additional remark. Experimental data are usually fitted with an Arrhenius relation, $k = A \exp(-E/k_B T)$. Customarily, the validity of the TST equation, Eq. 7, is assumed and H^\ddagger is replaced with $H^\ddagger - TS^\ddagger$, to extract activation enthalpy and entropy by means of the relations $H^\ddagger = E$ and $\exp(S^\ddagger/k_B) = (2\pi A/\omega_B)$. These approximations are based on the assumption that the transmission factor, κ , is nearly temperature-independent. Figure 4 shows, however, that κ depends on friction. Friction is strongly temperature-dependent. Thus, with the relation

$$\zeta \approx \zeta_0 \exp(E_i/k_B T)$$

the relation between activation enthalpies and entropies corresponding to the high-damping result Eq. 14 are (14, 32)

$$H^\ddagger - H^* = E_i, S^\ddagger - S^* = E_i/T_0 \quad (15)$$

where T_0 is the average temperature where the data were taken. These relations show that the intrinsic activation enthalpies and entropies are smaller than the ones extracted in the customary way from an Arrhenius fit. A similar caveat applies to the activation volume, as has been pointed out by Montgomery, Chandler, and Berne (28). Again the pre-exponential term can hide part of the pressure dependence. The relations shown in Eq. 15 are valid in the overdamped regime; closer to η_{crit} they must be modified (14). In very viscous solvents the overdamped motion in the transition state may be more rapid than that used in measuring macroscopic viscosities, and “memory” effects must be taken into account (33): Grote and Hynes have shown that one need only replace the low-frequency friction coefficient in the Kramers rate by its renormalized value at the overdamped frequency of motion in the transition state. Very viscous solvents have a power-law dependence of viscosity on frequency. Thus at high friction this argument leads to a fractional power-dependence on macroscopic viscosity, as has been observed in reactions of biomolecules (14, 34).

Friction and Criteria for Nonadiabaticity

So far we have treated the effect of friction on adiabatic transitions, a well-studied problem. Friction will also affect the nonadiabatic features of a reaction: it

may cause the system to spend more time in the transition region, which would allow more time for a change in electronic state. All three length scales, ℓ_{TS} , ℓ_{LZ} , and λ , are important in determining the dynamics, and we must discuss various limiting cases to see how they affect adiabaticity.

1) $\ell_{\text{LZ}} \gg \ell_{\text{TS}}$. In Fig. 3b, ℓ_{LZ} is approximately the region where the potential is within Δ of the col; ℓ_{TS} is the corresponding region with Δ replaced by $k_B T$. The condition $\ell_{\text{LZ}} \gg \ell_{\text{TS}}$ hence implies $\Delta \gg k_B T$; the higher electronic state is thermally inaccessible, and the reaction is adiabatic. Nonadiabatic effects are important only if $\ell_{\text{LZ}} \leq \ell_{\text{TS}}$.

2) $\ell_{\text{LZ}} \ll \ell_{\text{TS}} \ll \lambda$. Under these conditions, the higher energy state is thermally accessible, and each crossing of the transition region is ballistic. One obtains the rate coefficient by multiplying the TST rate coefficient by P , Eq. 3. In the limit $\gamma_{\text{LZ}} \ll 1$, the result is identical to the one derived from the Golden Rule and used by Jortner and Ulstrup (6) and by Redi *et al.* (7) to analyze CO binding to heme proteins. The corresponding adiabaticity parameter, Eq. 2, can be written as

$$\gamma_{\text{LZ}} = \ell_{\text{LZ}}^2 / \ell_{\text{dB}} \ell_{\text{TS}} \quad (16)$$

where $\ell_{\text{dB}} = \hbar/mv$ is the reduced thermal deBroglie wavelength.

3) $\ell_{\text{LZ}} \ll \lambda \ll \ell_{\text{TS}}$. On each passage through the transition region, multiple crossings of the mixing (Landau-Zener) region occur. Between crossings, but before dropping into one of the energy wells, the system passes into a region in which the energy gap is large. It is reasonable to assume that there is no phase memory between the crossings so that the probabilities of crossings add incoherently as in classical probability theory. The number of crossings is approximately given by $N_c = (\ell_{\text{TS}}/\lambda)$. If one assumes that the random number of successful crossings follows a Poisson distribution, the probability P of reaching the product surface becomes for $N_c \gg 1$:

$$P = \frac{1}{2} [1 - \exp(-\pi N_c \gamma_{\text{LZ}})] \quad (17)$$

Even if the parameter γ_{LZ} , Eq. 2, is small, the reaction may appear adiabatic since the relevant parameter

$$\tilde{\gamma}_{\text{LZ}} = N_c \gamma_{\text{LZ}} = (\ell_{\text{TS}}/\lambda) \gamma_{\text{LZ}} = \ell_{\text{LZ}}^2 / \ell_{\text{dB}} \lambda \quad (18)$$

can be large. By the same argument the adiabaticity parameter

$$\tilde{\gamma}_{\text{LZ}} = N_c \gamma_{\text{LZ}} = (\tau_E/\tau_r) \gamma_{\text{LZ}}$$

may be used in the low-damping regime. The nonadiabatic transmission factor

must be used in addition to the factor κ , which arises from the Brownian recrossings over the barrier. Thus, in the high-friction limit, one obtains the rate coefficient by multiplying the adiabatic diffusion-controlled rate, Eq. 14, by P . An interesting result is obtained if γ_{LZ} is small. The adiabatic rate coefficient then is decreased by the factor $(\lambda/\ell_{\text{TS}})$ because of multiple crossings, but the rate of surface crossing is increased by the factor $(\ell_{\text{TS}}/\lambda)$ because of the same multiple crossings. The net effect is a viscosity-independent rate coefficient, essentially the same as the Golden Rule-TST result.

The approach taken here is similar to the surface-hopping theory of Tully and Preston, to the treatment of electron transfer in proteins by Warshel, and to the treatment of iodine recombination by Ali and Miller (35). The results found here through a consideration of multiple-crossing effects have been obtained by Tembe, Friedman, and Newton by means of a chemical kinetic scheme in which attainment of the activated state is described by a rate equation and surface crossing is described as a subsequent step (36).

4) $\lambda \ll \ell_{\text{LZ}} \ll \ell_{\text{TS}}$. Under these conditions, the passage through the mixing region is not ballistic, and the Landau-Zener multiple-crossing argument is invalid. The system remains in the mixing region for quite some time. This case was analyzed by Zusman (37) with the stochastic Liouville equation. We can obtain his result through a simple physical argument. The most natural generalization of the small-splitting Landau-Zener result, Eq. 4, is to replace the constant thermal velocity v with an effective velocity for crossing the Landau-Zener region by diffusion. An uninterrupted ballistic passage through the distance ℓ_{LZ} takes $n_{\text{LZ}} = (\ell_{\text{LZ}}/\lambda)$ steps of length λ whereas diffusion requires n_{LZ}^2 steps; hence, $v_{\text{eff}} = (\lambda/\ell_{\text{LZ}})v$. The parameter $\lambda_{\text{LZ}}^{\text{eff}}$ characterizing one diffusive passage through the mixing region consequently is given by

$$\lambda_{\text{LZ}}^{\text{eff}} = (\ell_{\text{LZ}}/\lambda) \gamma_{\text{LZ}}$$

But we must bear in mind that since $\lambda \ll \ell_{\text{TS}}$ there will be $N_m = \ell_{\text{TS}}/\ell_{\text{LZ}}$ crossings of the mixing region while the system remains in the region of the transition state. This estimate for N_m is obtained in the same way as the estimate for N_c and takes into account that the Brownian path is statistically self-similar. The total adiabaticity factor consequently is given by

$$N_m \lambda_{\text{LZ}}^{\text{eff}} = (\ell_{\text{TS}}/\ell_{\text{LZ}}) (\ell_{\text{LZ}}/\lambda) \gamma_{\text{LZ}} = (\ell_{\text{TS}}/\lambda) \gamma_{\text{LZ}} = \tilde{\gamma}_{\text{LZ}}$$

The adiabaticity criterion is the same as given in Eq. 18 for case 3) and agrees with the criterion obtained by Zusman (37). The total transmission factor, according to this argument, monotonically decreases with friction.

The results of cases 1 through 4 are summarized in the plot of transmission factor versus friction, Fig. 4. Since there is no discontinuity in behavior as the mean free path becomes smaller than ℓ_{LZ} , this plot is basically the plot of Friedman and co-workers, which was based on kinetic considerations (36). When the adiabatic transmission factor is small, the number of crossings is large, and the rate is the same for both the nonadiabatic and adiabatic cases. When $N_c P \lesssim 1$, the number of crossings is insufficient to give enhanced adiabaticity, and the rate coefficient reaches a plateau given by the Landau-Zener result. Thus, for nonadiabatic reactions, the Landau-Zener theory represents an upper bound much like the one provided by TST for adiabatic reactions.

Preexponential Factors and the Adiabaticity Parameter

The relations obtained in the last three sections show how entropy, friction, and electronic structure affect the preexponential term in an Arrhenius expression and how friction can change the adiabaticity criterion. Friction and nonadiabaticity reduce the preexponential term, whereas entropy can either decrease it or increase it. Further information is obtained if transitions $A \rightarrow B$ and $B \rightarrow A$ are considered. Friction and nonadiabaticity reduce both preexponential terms A_{AB} and A_{BA} by the same factors, whereas the entropy contribution yields

$$\frac{A_{BA}}{A_{AB}} = \frac{\exp(S_{BA}^{\ddagger}/k_B)}{\exp(S_{AB}^{\ddagger}/k_B)} = \exp(S_A - S_B)/k_B \quad (19)$$

Entropy affects A_{BA} and A_{AB} differently. (In Eq. 19 we assume that $\omega_A = \omega_B$; if these frequencies differ, the difference will appear as an entropy contribution.)

The first clue to the importance of the various factors is the determination of both terms A_{AB} and A_{BA} . The ratio indicates if the entropy plays a major role. (Even if the ratio is unity, entropy still may be important.)

A second clue is given by the dependence of $k(T, \zeta)$ on friction (solvent viscosity) at constant temperature. If the rate is strongly viscosity-dependent, the data must be evaluated with the Kramers equations, and friction may be responsible for the reduction of the preexponential factor below the TST value. (In a

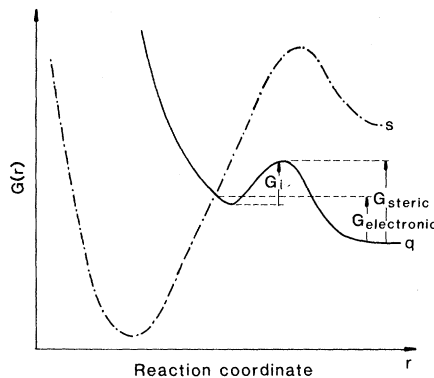


Fig. 5. Hypothetical energy surfaces in a protein. The diabatic energy curves of Fig. 3a are modified by the addition of a steric barrier. On the quintuplet energy surface, q, the steric barrier produces a metastable intermediate state.

protein, however, friction may play a role even if no dependence on the external solvent viscosity is present.)

If the rate depends on viscosity and if the preexponential factor is reduced below the TST value, the adiabaticity parameter γ_{LZ} is increased by the amount that the rate coefficient k is decreased. A transition that without friction is nonadiabatic can become adiabatic.

Scenarios for the Molecular Details of CO and O₂ Recombination

To apply the ideas contained in the previous sections, it is necessary to pin down some details of the topography of the potential surface and to obtain information about the character of the molecular motion at the active site. On both of these issues it is possible only to make educated guesses informed by quantum-chemical and spectroscopic investigations as well as data from the kinetics themselves. In accord with Ockham's razor, the simplest guess fitting the data will be used.

Some insight into the binding process comes from the first clue described in the previous section, the ratio A_{AB}/A_{BA} . The large value (approximately 10^6) of the experimental ratio implies that entropy plays a major role in the process, and in fact, it can account for the observed deviations of the preexponential factors from 10^{12} sec^{-1} . The second clue is negative evidence. The values listed in Table 1 are essentially independent of solvent viscosity. Since bond formation at the heme iron occurs deep within the protein, this clue is not conclusive; friction may still play a role in the process.

We can estimate values of the parameters ℓ_{TS} , ℓ_{LZ} , and λ . The width of the transition state, ℓ_{TS} , can be obtained from Eqs. 12a or 12b. Equation 12a

yields, for $T = 100 \text{ K}$, $m = 50 \text{ amu}$, and $\omega^*/2\pi = 3 \times 10^{12} \text{ sec}^{-1}$, $\ell_{TS} = 20 \text{ pm}$ ($1 \text{ \AA} = 100 \text{ pm}$). To extract a value from Eq. 12b, we assume that $|F_2 - F_1|$ is dominated by state B. Describing the energy well for B by

$$U_q(r - r_B) = \frac{1}{2} m \omega_B^2 (r - r_B)^2$$

we get

$$F_1 = \left. \frac{dU_1(r)}{dr} \right|_{r_0} = \frac{2}{r_B - r_0} U(r_0)$$

If we approximate $U(r_0)$ by the barrier height H_{BA}^{peak} (Table 1) and arbitrarily set $r_B - r_0 = 100 \text{ pm}$, we find for myoglobin, $F_1 = 2 \times 10^{-10} \text{ J m}^{-1}$, and hence, from Eq. 12a, $\ell_{TS} = 7 \text{ pm}$. As expected, ℓ_{TS} is larger for a parabolic barrier than for a cusp. It is worth noting that ℓ_{TS} is comparable to the root-mean-square fluctuations of the iron atom as observed by x-ray diffraction (38). The time it takes the system to ballistically cross the transition-state region is about 10^{-14} second .

The width ℓ_{LZ} of the Landau-Zener mixing region is very different for O₂ and CO. For O₂, we expect Δ to be given by a first-order spin-orbit interaction, since the Fe-O₂ system undergoes a spin change of 1. Using the estimates of Hopfield and co-workers (7), we get $\Delta(\text{O}_2) \approx 200 \text{ cm}^{-1} = 2.4 \text{ kJ mol}^{-1}$. For CO, a second-order spin-orbit interaction is required, and we take the value $\Delta(\text{CO}) \approx 10 \text{ cm}^{-1} = 0.12 \text{ kJ mol}^{-1}$ of Hopfield *et al.* With Eq. 1 and $|F_2 - F_1| \approx 2 \times 10^{-10} \text{ J m}^{-1}$, we get $\ell_{LZ}(\text{O}_2) = 20 \text{ pm}$ and $\ell_{LZ}(\text{CO}) = 1 \text{ pm}$. Inserting these values into Eq. 2 with $v = 130 \text{ m sec}^{-1}$ gives the adiabaticity parameters $\gamma_{LZ}(\text{O}_2) = 6$ and $\gamma_{LZ}(\text{CO}) = 10^{-2}$. The probability P , Eq. 3, would then be 1 for O₂, but 0.016 for CO. Oxygen should indeed bind adiabatically, and CO should bind at least 60 times slower. Since both processes are about equally fast, the binding process requires further scrutiny.

The arguments of the previous sections indicate that friction can render a transition with small splitting adiabatic. Arriving at a reliable value for ζ or λ is, however, fraught with uncertainties. The most direct study of velocity correlations in proteins comes from simulations of molecular dynamics (39). For large groups, such as the heme, these computations suggest that friction arises from a collisional mechanism, as in dense liquids. The rotation of a tyrosine ring, for instance, has a velocity relaxation time of $5 \times 10^{-14} \text{ second}$. This value corresponds, according to Eq. 11 to $\lambda = 7 \text{ pm}$. As an approximation, we assume that the motion of the tyrosine ring is similar

to the motion of the heme group governing CO binding. The ratio $\ell_{\text{TS}}/\lambda \approx 1$ implies that friction has little effect on the adiabaticity parameter; CO would still bind nonadiabatically. Mössbauer line shape studies on heme proteins have been interpreted, however, as indicating much larger frictional effects (40). Effective relaxation times of 5×10^{-16} second have been inferred, short enough to make the transition adiabatic. The interpretation of these effects by a collisional model is, however, untenable. A mechanism for large apparent frictional effects has been put forward by Parak and co-workers (40) and by Schulten (41). The mechanism is similar to sliding friction: what looks like a smooth (perhaps quadratic) potential surface may have hills and valleys that must be overcome. This effect makes the effective friction large. The time scale of escape from a single energy valley may be long enough to be undetected in a computer simulation of the molecular dynamics but short enough to contribute to the Mössbauer effect. Undulations in a potential surface in a protein could arise from coupling of the reaction coordinate to helices or side chains that can slide over each other as in incommensurate phases absorbed on a periodic substrate. Since ℓ_{TS} is comparable to the root-mean-square motion of the iron atom, the large amount of friction deduced from the Mössbauer effect may indeed play a role. A relaxation time of 5×10^{-16} second corresponds to $\lambda \approx 0.1$ pm and $\ell_{\text{TS}}/\lambda \approx 10^2$. Such a ratio would indicate that CO binding is adiabatic, and it would give $A_{\text{BA}} = 10^{10} \text{ sec}^{-1}$. Two aspects remain unexplained, however: the entropy of the transition state would be close to that of the initial state, and the opposite pressure dependence for O₂ and CO binding is not understood. We therefore turn to another, related, possibility that may explain all observed features.

Steric Control

The col in Fig. 3b occurs where the electronic energy levels cross. This coincidence is specific for two-body interactions where the “steric” features are directly coupled with the electronic ones because they are produced by the same interaction. In a many-body system, such as a protein, where many different components can move during a reaction, the coincidence is no longer guaranteed. The invisible protein coordinates can produce one or more intermediate states near the Landau-Zener mixing region (Fig. 5). In this hypothetical case, a steric contribution produces a bump on

both the singlet and the quintuplet energy surface. On the quintuplet curve, the steric interaction gives rise to an intermediate state. If the diabatic curves cross near the metastable intermediate state, the transition rate between the electronic curves can be increased. The increase can be understood by looking again at the argument leading to the adiabaticity parameter γ_{LZ} , Eq. 2. An intermediate state with barrier G_i will increase γ_{LZ} by lengthening the time τ_{LZ} that the system spends in the mixing region, $\tau_{\text{LZ}} = \tau_{\text{LZ}} \exp(G_i/k_{\text{B}}T)$. The kinetic analysis of Friedman and co-workers (36) would be most appropriate to such a situation. If friction is also present, the adiabaticity parameter becomes with Eq. 18

$$\gamma'_{\text{LZ}} = \gamma_{\text{LZ}} \left(\frac{\ell_{\text{TS}}}{\lambda} \right) e^{G_i/k_{\text{B}}T} \quad (20)$$

The large effective friction inferred from Mössbauer experiments and the existence of one or more intermediate states are probably related; both can be produced by a sliding friction mechanism. When CO binds, the iron moves toward the heme plane carrying with it the proximal histidine F8 (42). It would be advantageous for the F helix then to slide, just as it does in communicating allosteric information in hemoglobin. This motion could be strongly hindered, which would result in intermediate states. There is ample direct evidence for intermediates away from the transition state. These have been observed in the infrared studies of recombination (19) and in resonance Raman spectroscopy (43). In the Raman studies, the F helix has been implicated as the cause of these states. In accord with this idea are the observations that the barrier-height distribution for CO and O₂ binding, studied at low temperature, may be related to the large fluctuations of the F helix atoms found by spectroscopy (44), and that protein relaxation, after photodissociation, exhibits a nonexponential time dependence (45).

The combination of friction and intermediate states can change a nonadiabatic transition into an adiabatic one. An intermediate state may also explain the different pressure dependencies for CO and O₂ binding, because the avoided crossing of the diabatic energy surfaces may take place at different values of the reaction coordinate for CO and O₂. The observation that the pressure dependence for CO binding is very different in myoglobin and in protoheme and differs in sperm whale and horse myoglobin (17) also points to a strong influence of the protein on binding.

After having pointed out that CO and

O₂ bind very similarly and most likely on an adiabatic energy surface, we must add a word of caution. If binding were totally adiabatic and governed by exactly the same energy surface for CO and O₂, the pressure effect should be identical. The different pressure effect implies that the details of the energy surfaces exert some influence and cannot be totally disregarded. For CO binding, a Landau-Zener factor P somewhat smaller than unity cannot be excluded by the experimental data, and such a factor could explain the small differences observed in the binding of CO and O₂ as, for instance, shown in Fig. 2.

Future Avenues of Research

A knowledge of chemical reaction theory is the basis for understanding biological reactions. Since the complex and highly organized structure of biomolecules may affect chemical reactions profoundly, we are forced to study the effect of the surroundings on reactions. In this article, we have used one particularly well-investigated biological process, the binding of O₂ and CO to heme proteins, as a paradigm. The experimental data at low temperatures, where the binding of O₂ and CO to the heme iron occurs from within the heme pocket, indicate that the two electronically dissimilar ligands bind with nearly equal rates. Steric effects must play a larger role than anticipated. An analysis of the factors that can affect binding implies that friction and steric effects may play a far more important role in proteins than in simpler systems. The lessons learned from this analysis may be applied to other systems and reactions, such as electron transfer in photosynthesis and respiration.

Both the experimental and the theoretical work discussed here are only a beginning. More experiments are needed to establish a database broad enough for more detailed analysis. The experiments should include additional ligands, additional proteins, and far more detailed studies of the effect of pressure and magnetic fields. The theoretical approaches also must be extended. Most quantum-chemical studies have concentrated on electronic states near the equilibrium geometry. Much more complete calculations of electronic states near the crossing points need to be undertaken since intermediate states may arise from steric effects in the protein. If successful, these studies will teach us more about reaction theory. They will also tell us how the functions of proteins are controlled and adjusted through a combination of electronic and steric factors.

References and Notes

- S. Glasstone, K. J. Laidler, H. Eyring, *The Theory of Rate Processes* (McGraw-Hill, New York, 1941).
- B. Chance *et al.*, Eds., *Tunneling in Biological Systems* (Academic Press, New York, 1979).
- V. I. Goldanskii, *Chem. Scr.* **13**, 1 (1978).
- N. Alberding *et al.*, *Science* **192**, 1002 (1976); J. O. Alben *et al.*, *Phys. Rev. Lett.* **44**, 1157 (1980).
- J. Ulstrup, *Charge Transfer Processes in Condensed Media* (Springer-Verlag, New York, 1979); D. DeVault, *Q. Rev. Biophys.* **13** (No. 4), 387 (1980); N. Sutin, *Acc. Chem. Res.* **15**, 275 (1982).
- J. Jortner and J. Ulstrup, *J. Am. Chem. Soc.* **101**, 3744 (1979).
- M. H. Redi, B. S. Gerstman, J. J. Hopfield, *Biochem. J.* **35**, 471 (1981).
- R. H. Austin *et al.*, *Biochemistry* **14**, 5355 (1975).
- W. Doster *et al.*, *ibid.* **21**, 4831 (1982).
- A. B. P. Lever and H. B. Gray, Eds., *Iron Porphyrins* (Addison-Wesley, Reading, Pa., 1983).
- W. A. Goddard III and B. D. Olafson, in *Quantum Chemistry in Biomedical Sciences* (New York Academy of Science, New York, 1981), pp. 419-433.
- N. Alberding *et al.*, *Biochemistry* **17**, 43 (1978).
- D. D. Dlott *et al.*, *Proc. Natl. Acad. Sci. U.S.A.* **80**, 6239 (1983).
- D. Beece *et al.*, *Biochemistry* **19**, 5147 (1980).
- E. A. Moelwyn-Hughes, *Physical Chemistry* (Pergamon, Oxford, 1961), pp. 431-435.
- J. P. Collman, J. I. Brauman, K. S. Suslick, *J. Am. Chem. Soc.* **97**, 7185 (1975).
- N. A. Alberding, thesis, University of Illinois, Urbana-Champaign (1978); L. B. Sorensen, thesis, University of Illinois at Urbana-Champaign, (1980).
- B. B. Hasinoff, *Biochemistry* **13**, 3111 (1974); E. F. Caldin and B. B. Hasinoff, *J. Chem. Soc. Faraday Trans. 1* **71**, 515 (1975).
- J. O. Alben *et al.*, *Proc. Natl. Acad. Sci. U.S.A.* **79**, 3744 (1982).
- L. D. Landau and E. M. Lifshitz, *Quantum Mechanics* (Pergamon, London, 1958), pp. 304-312; W. Kauzmann, *Quantum Chemistry* (Academic Press, New York, 1957).
- E. J. Heller and R. C. Brown, *J. Chem. Phys.* **79**, 3336 (1983).
- L. Landau, *Sov. Phys.* **1**, 89 (1932); *Z. Phys. Sov. 2*, 1932 (1932).
- C. Zener, *Proc. R. Soc. Ser. A* **137**, 696 (1932).
- E. G. C. Stueckelberg, *Helv. Phys. Acta* **5**, 369 (1932).
- A. Einstein, *Ann. Phys. (Leipzig)* **19**, 371 (1906); R. Kubo, *Rep. Progr. Phys.* **29**, 255 (1966); D. A. MacQuarrie, *Statistical Mechanics* (Harper and Row, New York, 1976).
- H. A. Kramers, *Physica (Utrecht)* **7**, 284 (1940).
- H. C. Brinkman, *ibid.* **22**, 149 (1956); R. Landauer and J. A. Swanson, *Phys. Rev.* **121**, 1668 (1956).
- J. S. Langer, *Phys. Rev. Lett.* **21**, 973 (1968); E. Helfand, *J. Chem. Phys.* **54**, 4651 (1971); B. Widom, *ibid.* **55**, 44 (1971); C. Blomberg, *Physica (Utrecht)* **86A**, 49 (1977); N. G. van Kampen, *J. Stat. Phys.* **17**, 71 (1977); J. L. Skinner and P. G. Wolynes, *J. Chem. Phys.* **69**, 2143 (1978); J. R. Montgomery, D. Chandler, B. J. Berne, *ibid.* **70**, 4065 (1979); R. F. Grote and J. T. Hynes, *ibid.* **74**, 4465 (1981); P. Hänggi and H. Thomas, *Phys. Rep.* **88**, 207 (1982); B. Carmeli and A. Nitzan, *J. Chem. Phys.* **79**, 393 (1983); *Phys. Rev. A* **29**, 1481 (1984); M. M. Büttiker, E. P. Harris, R. Landauer, *Phys. Rev. B* **28**, 1268 (1983).
- S. Mashimo, *Macromolecules* **9**, 91 (1976); D. L. Hasha, T. Eguchi, J. Jonas, *J. Chem. Phys.* **75**, 1570 (1981); *J. Am. Chem. Soc.* **104**, 2290 (1982); S. P. Velsko and G. R. Fleming, *Chem. Phys.* **65**, 59 (1982); S. P. Velsko, D. H. Waldeck, G. R. Fleming, *J. Chem. Phys.* **78**, 249 (1983); K. M. Keery and G. R. Fleming, *Chem. Phys. Lett.* **93**, 322 (1982); G. Rothenberger, D. K. Negy, R. M. Hochstasser, *J. Chem. Phys.* **79**, 5360 (1983).
- D. G. Truhlar, W. L. Hase, J. T. Hynes, *J. Phys. Chem.* **87**, 2664 (1983).
- M. Büttiker and R. Landauer, *Phys. Rev. Lett.* **52**, 1250 (1984); B. Carmeli and A. Nitzan, *ibid.*, p. 1251.
- B. Gavish and M. M. Werber, *Biochemistry* **18**, 1269 (1979).
- R. F. Grote and J. T. Hynes, *J. Chem. Phys.* **76**, 2715 (1981); *ibid.* **75**, 2191 (1981); *ibid.* **77**, 3736 (1982); P. Hänggi and F. Mojtabai, *Phys. Rev. A* **26**, 1168 (1982); P. Hänggi, *J. Stat. Phys.* **30**, 401 (1983).
- D. Beece *et al.*, *Photochem. Photobiol.* **33**, 517 (1981).
- J. C. Tully and R. K. Preston, *J. Chem. Phys.* **55**, 262 (1971); A. Warshel, *J. Phys. Chem.* **86**, 2218 (1982); D. P. Ali and W. H. Miller, *J. Chem. Phys.* **78**, 6640 (1983).
- B. L. Tembe, H. L. Friedman, M. D. Newton, *J. Chem. Phys.* **76**, 1490 (1982); H. L. Friedman and M. Newton, *Faraday Discuss. Chem. Soc.* **74**, 73 (1982).
- L. D. Zusman, *Chem. Phys.* **49**, 295 (1980).
- H. Frauenfelder, G. A. Petsko, D. Tsernoglou, *Nature (London)* **280**, 558 (1979).
- J. A. McCammon and M. Karplus, *Annu. Rev. Phys. Chem.* **31**, 29 (1980); J. A. McCammon, P. G. Wolynes, M. Karplus, *Biochemistry* **18**, 927 (1979).
- F. Parak, E. W. Knapp, D. Kucheida, *J. Mol. Biol.* **161**, 177 (1982); E. W. Knapp, S. F. Fischer, F. Parak, *J. Chem. Phys.* **78**, 4701 (1983).
- W. Nadler and K. Schulten, *Phys. Rev. Lett.* **51**, 1712 (1983).
- R. E. Dickerson and I. Geis, *Hemoglobin: Structure, Function, Evolution and Pathology* (Benjamin Cummings, Menlo Park, Calif., 1983).
- J. M. Friedman *et al.*, *J. Biol. Chem.* **258**, 10564 (1983).
- H. Frauenfelder, in *Structure, Dynamics, Interactions and Evolution of Biological Macromolecules*, C. Hélène, Ed. (Reidel, Dordrecht, 1983), pp. 227-239.
- _____, in *Structure and Dynamics of Nucleic Acids, Proteins, and Membranes*; E. Clementi, G. Corongiu, M. H. Sarma, R. H. Sarma, Eds. (Adenine, New York, 1985), pp. 205-217.
- Supported in part by NSF grants PCM82-09616 and CHE81-22012 and NIH grant HHS-PHS GM 18051. We enjoyed helpful discussions with J. S. Langer and J. R. Schrieffer and we thank A. Ansari, M. M. Büttiker, R. Cline, and T. Sauke for their help and critical remarks.

RESEARCH ARTICLE

Constitutive and Conditional Suppression of Exogenous and Endogenous Genes by Anti-Sense RNA

Jonathan G. Izant and Harold Weintraub

In order to study the biological functions associated with cloned gene sequences, we previously designed a strategy for specifically inhibiting their expression *in vivo* (1). We used, as a test system, the herpes simplex virus (HSV) thymidine kinase (TK) gene in plasmid DNA constructions designed to transcribe the anti-sense (noncoding) DNA strand. The anti-sense transcript has a sequence complementary to the target messenger RNA (mRNA) and can presumably anneal with the mRNA and disrupt normal processing or translation. The anti-sense TK plasmid is constructed *in vitro* by inverting the TK protein-

coding sequence with respect to its promoter. Such a plasmid will specifically inhibit expression of the cognate sense TK plasmid after both plasmids are microinjected into LTK⁻ cells (1). The promising results with the HSV-TK model system suggest that anti-sense RNA can provide an additional methodology for genetic analysis in eukaryotic systems that are not readily amenable to standard mutational analysis. Inhibition of function by anti-sense RNA is a regulatory strategy in prokaryotes where it has been found to control translation (2) as well as the activity of RNA primers for initiating episome DNA replication

(3). Similar mechanisms have not yet been described in eukaryotes.

We have now extended the use of anti-sense inhibition to both transient and stable DNA-mediated transformation systems. We show that a fragment as short as 52 bases of 5' untranslated anti-sense TK RNA inhibits TK activity. The inhibition is sequence specific. Anti-sense herpes TK inhibits sense herpes TK, but not expression from the non-cross-hybridizing chicken TK gene, while anti-sense chicken TK inhibits expression from a sense chicken TK plasmid, but not from a sense herpes TK plasmid. Conditional, dexamethasone-inducible, anti-sense inhibition is demonstrated by the use of the long terminal repeat (LTR) of the murine mammary tumor virus (MMTV) to direct the synthesis of anti-sense TK RNA. We show that a stably introduced TK gene is also inhibited by anti-sense TK, and finally that expression of the normal endogenous cytoplasmic actin gene can be inhibited by anti-sense actin expression plasmid constructions. The actin inhibition is detected as a diminution of the actin microfilament array and as a decrease in cell viability.

J. G. Izant and H. Weintraub are in the Department of Genetics, Fred Hutchinson Cancer Research Center, Seattle, Washington 98104.